



# Liver Anatomy of Long-Eared Hedgehog (*Hemiechinus auritus*) Using Multimodal Imaging

Mahdi Ghanaat Pishesh<sup>1</sup> , Mohammad Nasrollahzadeh Masouleh<sup>1\*</sup> , Hassan Gilanpour<sup>2</sup> , Saied Bokaie<sup>3</sup> ,  
and Siamak Mashhadirafiee<sup>1</sup> 

<sup>1</sup>Department of Clinical Sciences, SR.C., Islamic Azad University, Tehran, Iran

<sup>2</sup>Department of Basic Sciences, SR.C., Islamic Azad University, Tehran, Iran

<sup>3</sup>Department of Epidemiology and Zoonosis, Faculty of Veterinary Medicine, University of Tehran, Tehran, Iran

\*Corresponding author's Email: 2594205443@iau.ir

## ABSTRACT

The long-eared hedgehog (*Hemiechinus auritus*), a small insectivorous species commonly encountered in exotic animal practice, lacks established imaging references for liver anatomy. The present study aimed to characterize the liver of clinically healthy adult animals using radiography, ultrasonography, computed tomography (CT), and magnetic resonance imaging (MRI). Seven clinically healthy adult one-year-old male hedgehogs with body weights of 320-410 grams were examined at the Diagnostic Imaging Unit of the Faculty of Veterinary Medicine, Islamic Azad University, Tehran, Iran. Radiography identified hepatic position and overall shape, while ultrasonography provided real-time assessment of parenchymal echotexture, gallbladder morphology, and major vascular landmarks. The CT and MRI provided detailed cross-sectional visualization, including morphometric measurements and evaluation of parenchymal and vascular architecture. Across all imaging techniques, the right and left hepatic lobes exhibited comparable dimensions and tissue characteristics, with no statistically significant morphometric differences between lobes. The present study established a preliminary reference for liver anatomy in *Hemiechinus auritus* using multimodal imaging, thereby facilitating clinical diagnosis in this species.

**Keywords:** Hedgehog, Liver, MRI, Radiography, Ultrasonography

## INTRODUCTION

The long-eared hedgehog (*Hemiechinus auritus* [*H. auritus*]), a popular exotic companion animal, has attracted attention for its distinctive physiological characteristics, including a desert-adapted metabolic profile, seasonal hibernation behavior, and an insectivorous diet (Juan-Sallés and Garner, 2007). Similar to other small exotic mammals, hedgehogs are prone to hepatic disorders that may progress to systemic illness if not detected early (Ballard and Cheek, 2016). The most frequently reported hepatic abnormalities in hedgehogs included hepatic lipidosis, inflammatory hepatopathies, and metabolic hepatic dysfunction (Juan-Sallés and Garner, 2007). Considering the liver's vital functions in detoxification, metabolic regulation, and nutrient storage, accurate anatomical characterization is essential for effective clinical diagnosis and management (Capello and Lennox, 2013; Bexton, 2016).

Although the hepatic disease is clinically significant in hedgehogs, there are still limited species-specific anatomical studies for assessing the normal liver in the long-eared hedgehog. Most available information on hedgehog visceral anatomy is based on general veterinary literature or from pathological reports and imaging studies of other small mammals, such as African hedgehogs (*Atelerix albiventris*), rabbits, chinchillas, and ferrets (Juan-Sallés and Garner, 2007; Ballard and Cheek, 2016). Although comparative anatomical and imaging data derived from other small exotic mammals, including African hedgehogs, rabbits, chinchillas, and ferrets, provide proper context, anatomical variation between species limits their direct relevance to *H. auritus*, particularly for organs such as the liver, which is sensitive to metabolic and physiological differences.

Previous imaging and anatomical investigations in small exotic mammals have demonstrated that hepatic morphology, lobar proportions, and spatial relationships with adjacent organs may differ considerably among species and body conformations (Capello and Lennox, 2013; von Stade and Sadar, 2024). However, imaging-based descriptions of normal liver anatomy in *H. auritus* are lacking, and no comprehensive reference framework integrating radiography,

ORIGINAL ARTICLE  
Received: October 07, 2025  
Revised: November 11, 2025  
Accepted: December 10, 2025  
Published: December 31, 2025

ultrasonography, computed tomography (CT), and magnetic resonance imaging (MRI) has been established for this species.

Advanced cross-sectional imaging techniques have improved the ability to illustrate hepatic lobar structure, vascular arrangements, and parenchymal features in different exotic mammals (Nabipour and Dehghani, 2012). Without baseline reference data for *H. auritus*, interpreting hepatic imaging results in clinical practice is difficult, especially when animals show nonspecific systemic signs. Defining standard, species-specific imaging features of the liver is crucial for enhancing diagnostic precision, informing clinical choices, and aiding comparative and translational investigation in exotic veterinary medicine. Therefore, the present study aimed to provide a comprehensive, descriptive multimodal imaging evaluation of liver anatomy in *H. auritus*, establishing essential reference data for clinical and study use.

## MATERIALS AND METHODS

### Ethical statement

The present study was conducted in accordance with national and international ethical standards for animal research and was approved by the Animal Ethics Committee of the Islamic Azad University, Science and Research Branch, Tehran, Iran (approval code: IR.IAU.SRB.REC.1403.338). All procedures were designed to minimize stress and avoid unnecessary harm. Only the sedation required for diagnostic imaging was performed; no invasive interventions were conducted. No animals were euthanized during or after the study, and all hedgehogs recovered fully following imaging. The study adhered to institutional, national, and international guidelines for the humane care and use of animals in research.

### Animals

The study comprised seven clinically healthy, 1-year-old male *H. auritus* hedgehogs, with body weights ranging from 320 to 410 g. The hedgehogs were obtained from licensed wildlife rehabilitation centers located in the South Khorasan and Sistan-Baluchestan provinces of Iran, regions within the natural distribution of *H. auritus*. Each hedgehog underwent a complete physical examination, including visual inspection, palpation, and preliminary abdominal radiographic screening, to confirm the absence of systemic, gastrointestinal, or urinary abnormalities, in accordance with standard diagnostic guidelines for small exotic mammals (Capello and Lennox, 2013).

The animals were housed individually in stainless steel enclosures measuring 60 × 45 × 45 cm, maintained at a temperature of 20-25°C, with a relative humidity of 40-60%, and exposed to a 12-hour light/dark cycle. All hedgehogs were fed a commercially formulated insectivore/exotic-mammal diet (VetLife Exotic Diet, Italy), with *ad libitum* access to fresh water. Environmental enrichment was provided to reduce stress and encourage natural behaviors, including opaque shelters, nesting material, PVC tunnels, and a shallow digging substrate.

Ethical restrictions on anesthesia for advanced imaging and the limited availability of healthy adult *H. auritus* necessitated a sample size of seven animals for the present study. The sample size was considered appropriate for descriptive anatomical and diagnostic imaging investigations and was consistent with the guidelines of Animal Research Reporting of *in vivo* Experiments (ARRIVE) for establishing preliminary baseline morphologic reference data in rare or protected species.

### Anesthesia procedure

To minimize stress and to ensure adequate immobilization during imaging, all hedgehogs were anesthetized using ketamine (20 mg kg<sup>-1</sup>, intramuscular; Alfasan, Woerden, Netherlands) combined with diazepam (2 mg kg<sup>-1</sup>, intramuscular; Caspian Tamin Pharmaceutical Co., Tehran, Iran). Physiological parameters, including heart rate, respiratory rate, peripheral oxygen saturation (SpO<sub>2</sub>), mucous membrane color, and palpebral and pedal reflexes, were continuously monitored using a multiparameter veterinary monitor (CMS8000VET, Contec Medical Systems Co., Qinhuangdao, China). Normal physiologic ranges and anesthetic safety criteria were interpreted in accordance with established guidelines for hedgehog and small exotic mammal anesthesia (Bexton, 2016; Hawkins et al., 2020).

Supplemental anesthesia was administered only when necessary. Additional ketamine (5 mg kg<sup>-1</sup>, intramuscular) was administered when clinical signs indicated inadequate anesthesia, such as partial return of withdrawal reflexes, reduced muscle relaxation, spontaneous limb movements, or purposeful reactions during imaging.

All hedgehogs were deprived of feed for 12 hours and water for 2 hours prior to anesthesia to mitigate the risk of regurgitation aspiration, following standard anesthetic safety recommendations for small exotic mammals. Following imaging, animals were moved to heated recovery enclosures and carefully monitored until they restored normal posture, coordinated movement, and full responsiveness. No adverse reactions or complications related to anesthesia were observed in any of the animals.

### **Radiography procedure**

Radiographic evaluation was performed to assess the position and relative radiodensity of the liver within the abdomen. All imaging was conducted at the Diagnostic Imaging Unit of the Faculty of Veterinary Medicine, Science and Research Branch, Islamic Azad University, Tehran, Iran. Animals were positioned in dorsal recumbency for ventrodorsal projections and in right lateral recumbency for lateral projections.

Radiographs were obtained using a CR Fuji computed radiography system (Fujifilm Corporation, Tokyo, Japan). Exposure parameters were optimized for small exotic mammals, with mean exposure settings of 55 kVp and 3.5 mAs, consistent with published radiographic techniques for exotic companion mammals (Capello and Lennox, 2013). All radiographic studies were reviewed by a board-certified veterinary radiologist. Animals were excluded from further imaging upon detection of any abnormality potentially affecting liver assessment. The mentioned abnormalities included hepatomegaly, irregular or rounded hepatic margins, peritoneal effusion, abdominal mineralization, gastrointestinal issues, or thoracic abnormalities. Radiographs served as the baseline reference for evaluating liver location, structure, and radiodensity compared to the surrounding organs.

### **Ultrasound procedure**

Ultrasonography was conducted in the Diagnostic Imaging Unit of the Faculty of Veterinary Medicine, Islamic Azad University (Tehran, Iran), using a Mindray S9 veterinary ultrasound system (Mindray Medical International Ltd., Shenzhen, China) equipped with a 7-12 MHz high-frequency linear transducer. The cranial abdominal region was clipped, and acoustic coupling gel was applied to optimize sound transmission and reduce surface artifacts. Scans were performed through the intercostal spaces and the subxiphoid window to obtain a comprehensive visualization of the liver parenchyma. Gain, depth, and focal settings were adjusted manually for each animal to optimize contrast resolution and delineation of hepatic and vascular structures. Animals were placed in dorsal and right-lateral recumbency to obtain standardized longitudinal and transverse images. A consistent morphometric protocol was applied. Hepatic length was measured in a longitudinal plane from the diaphragmatic surface to the caudal parenchymal margin. The caudal landmark for the right lobe was the cranial pole of the right kidney, while the caudal boundary of the left lobe was located near the lesser curvature of the stomach. Hepatic width was measured in the transverse plane at the level of the main portal vein bifurcation, using the maximal medial-to-lateral parenchymal dimension. All measurements were taken at end-expiration to minimize respiratory motion and were repeated three times by the same experienced examiner; the mean of the three measurements was used for analysis to minimize operator variability.

The gallbladder, intrahepatic vasculature, and major portal venous branches were qualitatively assessed for morphology, echogenicity, wall definition, and anatomical relationships. Hepatic margins, lobar echotexture patterns, and portal vein clarity were documented to establish baseline ultrasonographic characteristics of the healthy long-eared hedgehog.

### **Computed tomography procedure**

Computed tomography was performed in the Diagnostic Imaging Unit of the Faculty of Veterinary Medicine, Islamic Azad University (Tehran, Iran), using a dual-detector CT scanner (Siemens Healthineers, Erlangen, Germany). Animals were positioned in dorsal and sternal recumbencies to achieve consistent abdominal cross-sectional images.

For contrast-enhanced studies, iohexol (Omnipaque™ 300 mg I/mL; GE Healthcare, Chicago, USA) was administered intravenously at a dosage of 600 mg iodine/kg body weight, equivalent to 2 mL/kg of this formulation. The dosing protocol aligned with published CT contrast studies in small exotic mammals, including chinchillas and ferrets, where non-ionic iodinated contrast media were used at similar volume-based doses (Karakurum *et al.*, 2024; von Stade and Sadar, 2024). Scanning started about 25-30 seconds after the contrast was given, which was chosen to match the early portal venous phase. The timing helps ensure that the liver tissue and intrahepatic structures are properly highlighted vasculature. CT images were acquired at a slice thickness of 1.0 mm. High-frequency reconstruction algorithms optimized for soft-tissue evaluation were applied. The datasets were processed using Vitrea vital advanced visualization software (version 6.3.2160; Vital Images, Inc., Minnetonka, USA), which enabled three-dimensional (3D) reconstruction of the hepatic structures. The 3D reconstructions were used to evaluate overall hepatic morphology, delineate hepatic lobe boundaries, and assess spatial relationships between the liver and adjacent abdominal organs.

### **Magnetic resonance imaging procedure**

Magnetic resonance imaging was performed in the Diagnostic Imaging Unit of the Faculty of Veterinary Medicine, Islamic Azad University (Tehran, Iran), using a 1.5-T MRI system (Philips Achieva; Philips Healthcare, Best, Netherlands). All animals were positioned in dorsal recumbency, and imaging was performed with a small-animal surface coil to maximize signal-to-noise ratio.

T2-weighted fast spin-echo (T2-W) images, which provide enhanced sensitivity to differences in tissue water content, were obtained in the axial plane with repetition time (TR) at 3027 ms, echo time (TE) at 100 ms, slice thickness at 2.0 mm, field of view (FOV) at  $80 \times 80$  mm, matrix size at  $256 \times 256$ , number of excitations (NEX) at 3, bandwidth of 180 Hz/pixel, and slice spacing at 0 mm (contiguous slices). Additional T1-weighted and T2-weighted sequences were acquired in axial and coronal planes using TR at 597 ms, TE at 15 ms, slice thickness at 2.0 mm, FOV at  $80 \times 80$  mm, matrix size at  $256 \times 256$ , NEX at 3, and bandwidth of 180 Hz/pixel. The acquired sequences provided complementary anatomical information and were used to characterize hepatic margins, delineate hepatic lobe boundaries, and visualize intrahepatic vascular structures. For contrast-enhanced MRI examinations, a gadolinium-based contrast agent (gadopentetate dimeglumine; Magnevist®, Bayer HealthCare, Berlin, Germany) was administered intravenously at a dose of 0.1 mmol/kg body weight. Contrast-enhanced T1-weighted images were acquired approximately 20-30 seconds after contrast administration to achieve early vascular and parenchymal enhancement. The contrast agent and dosage were chosen according to well-established, weight-based MRI protocols commonly used across mammalian species, since there are currently no MRI contrast studies specific to hedgehogs (Islam and Tsnobiladze, 2024).

MRI datasets were evaluated qualitatively based on hepatic parenchymal signal intensity relative to skeletal muscle and subcutaneous fat. Quantitative morphometric measurements, including hepatic lobe length and width, were obtained from isotopically reconstructed MRI volumes using standardized anatomical landmarks consistent with those applied in the CT analysis.

### Image analysis

All CT and MRI datasets were reconstructed into 3D volumes and independently evaluated by two experienced veterinary radiologists, each with over five years of diagnostic imaging experience. Radiologists examined all CT and MRI datasets without separating the modalities, ensuring a consistent cross-modality approach. The CT datasets were analyzed using Vitrea Vital advanced visualization software (version 6.3.2160; Vital Images, Inc., Minnetonka, USA), which was also used for 3D reconstruction and quantitative morphometric measurements. MRI measurements were performed using the integrated measurement tools of the Philips Achieva workstation software (Philips Healthcare, Best, Netherlands). Quantitative variables included hepatic lobe dimensions and parenchymal attenuation values on CT, expressed in Hounsfield units. The MRI variables included qualitative signal intensity relative to skeletal muscle and subcutaneous fat. Additional qualitative assessments included intrahepatic vascular branching patterns, gallbladder position, hepatic capsule morphology, and lobar boundary definition. To assess measurement consistency, inter-observer reliability was quantified using a two-way random-effects intraclass correlation coefficient (ICC) with absolute agreement. The ICC values for hepatic lobe length and width were 0.87-0.94, indicating excellent agreement. Where measurements disagreed or discrepancies exceeded 10%, both radiologists reassessed the datasets to reach a consensus value, which was used in the final analysis.

### Statistical analysis

Statistical analyses were conducted using SPSS software (version 26.0; IBM Corp., Chicago, USA). Results were reported as mean  $\pm$  standard deviation (SD). Because of the small sample size ( $n = 7$ ), data for each variable were first tested for normal distribution using the Shapiro-Wilk test to confirm whether parametric methods were appropriate. All measured variables met the normality assumptions, allowing paired-sample t-tests to compare the right and left hepatic lobes within each imaging modality. A p-value less than 5% ( $p < 0.05$ ) was considered statistically significant. Given the exploratory nature of the study and limited sample size, statistical outcomes were interpreted cautiously. As a secondary confirmatory analysis, non-parametric Wilcoxon signed-rank tests were also performed. The mentioned tests produced results consistent with the findings of the paired t-test. To avoid overinterpretation, all statistical conclusions were evaluated in conjunction with qualitative and descriptive imaging findings.

## RESULTS

### Radiography

Radiographic imaging provided clear visualization of the liver and its anatomical connection to the nearby organs in the long-eared hedgehog. The liver was consistently observed in the cranial abdomen, extending caudally from the diaphragm toward the stomach. The right hepatic lobe was positioned near the caudal margin of the diaphragm, while the left hepatic lobe was located more ventrally, near the gastric curvature. Both ventrodorsal and right lateral projections demonstrated smooth, well-defined hepatic margins with sufficient contrast to distinguish the liver from neighboring soft-tissue organs, including the stomach, intestines, and diaphragm (Figure 1).

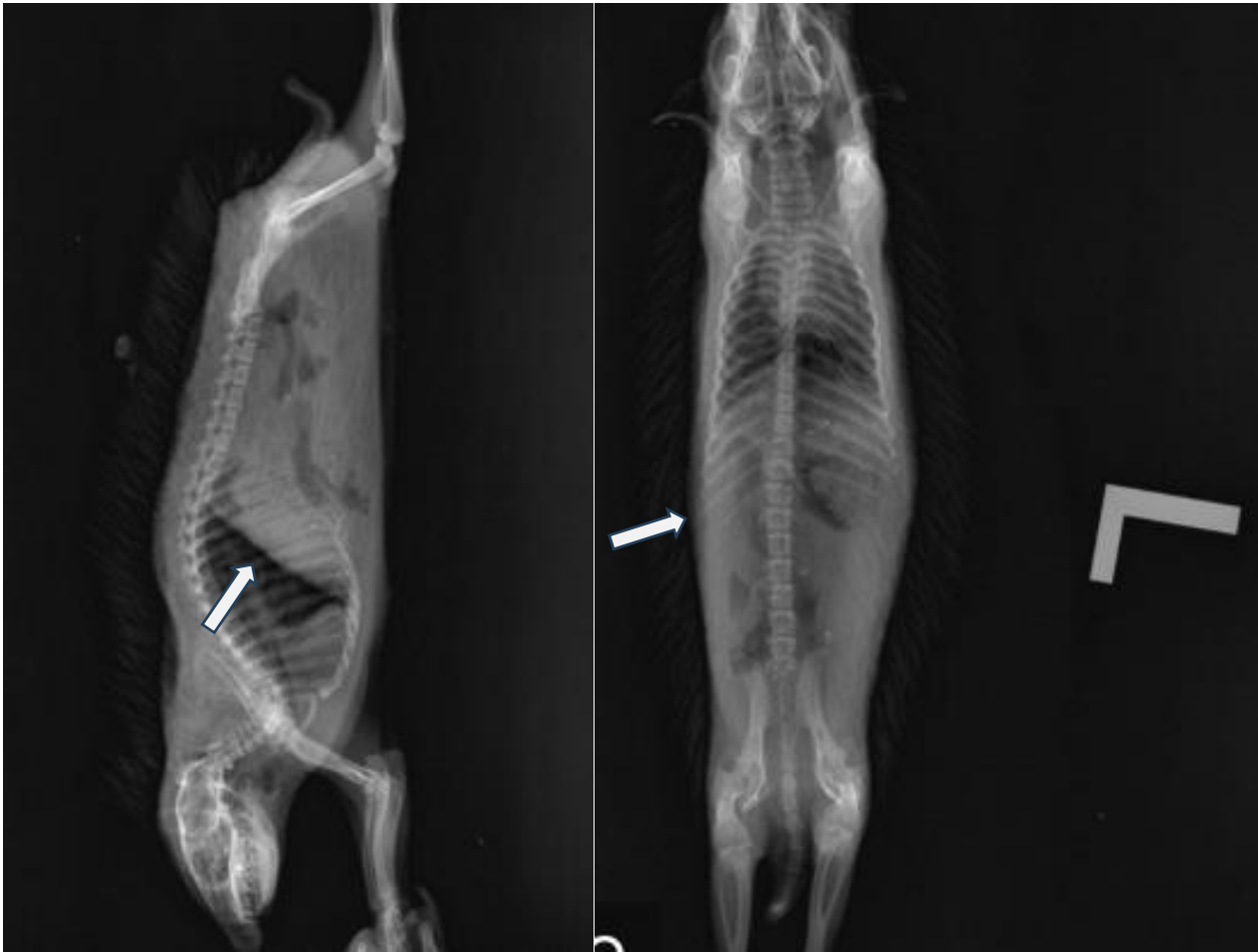


**Figure 1.** Right lateral (left) and ventrodorsal (right) radiographic views of an adult male long-eared hedgehog (*Hemiechinus auritus*; mean body weight 365 g). Arrows indicate the liver, visualized as a soft-tissue opacity in the cranial abdomen.

### Ultrasonography

Ultrasonographic assessment produced high-resolution images with clearly delineated hepatic parenchymal structure. Overall, the hepatic parenchyma appeared homogeneous in both lobes. Quantitative ultrasonographic measurements of hepatic length and width for the right and left lobes are summarized in Table 1 and indicate no statistically significant differences between lobes ( $p > 0.05$ ). Minor subjective echogenic variation was occasionally observed between lobes; however, the differences were subtle, inconsistent across individuals, and not associated with any measurable differences in shape or structure. The gallbladder was consistently visualized as an anechoic, thin-walled, fluid-filled sac situated along the visceral surface of the liver (Figure 2). Major vascular structures, including branches of the portal vein and hepatic veins, were easily identified and displayed typical anechoic lumens with well-defined echogenic walls (Figure 2). Hepatic margins were smooth and clearly defined, and no focal parenchymal abnormalities or biliary dilatation were observed.

**Table 1.** Morphometric measurements of the liver in long-eared hedgehogs (*Hemiechinus auritus*) across imaging techniques

Modality	Liver lobe	Length (cm)	Width (cm)	p-value (Length)	p-value (Width)
Radiography	Right	2.15 ± 0.22	1.28 ± 0.10	0.284	0.317
	Left	2.22 ± 0.25	1.31 ± 0.11		
Ultrasound	Right	2.20 ± 0.24	1.30 ± 0.12	0.301	0.355
	Left	2.27 ± 0.26	1.33 ± 0.13		
CT	Right	2.18 ± 0.20	1.29 ± 0.11	0.265	0.298
	Left	2.24 ± 0.22	1.32 ± 0.12		
MRI	Right	2.16 ± 0.21	1.27 ± 0.10	0.290	0.341
	Left	2.23 ± 0.23	1.30 ± 0.12		

Note: Values represent mean ± standard deviation (SD). Length and width measurements were obtained using standardized anatomical landmarks specific to each imaging modality. P-values indicate paired comparisons between right and left hepatic lobes within each modality.

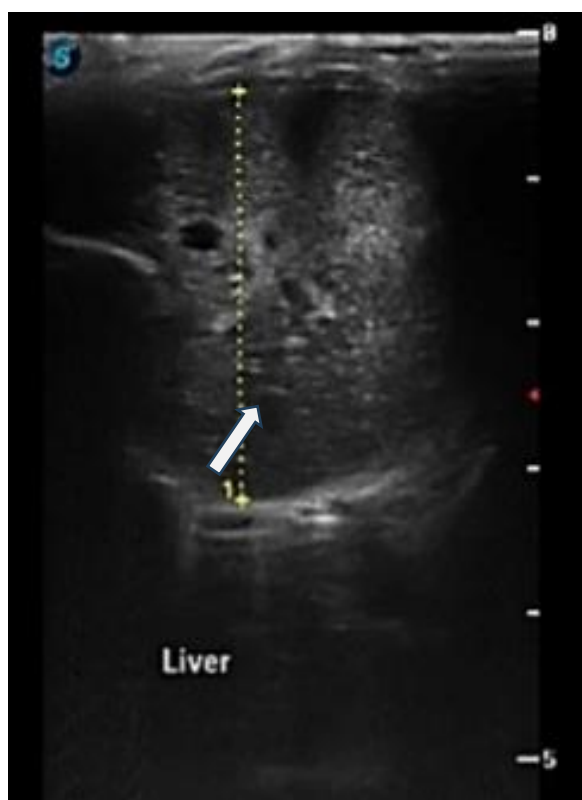


**Figure 2.** Ultrasonographic image of the liver in an adult male long-eared hedgehog (*Hemiechinus auritus*; aged one year old). The arrow indicates the hepatic parenchyma, showing a homogeneous echotexture.

### Computed tomography

Computed tomography provided detailed morphometric and volumetric information for the hepatic lobes of the long-eared hedgehog. The right hepatic lobe was consistently positioned near the caudate lobe, whereas the left hepatic lobe was situated closer to the spleen. Across all CT assessments, the right hepatic lobe measured  $2.18 \pm 0.20$  cm in length and  $1.29 \pm 0.11$  cm in width, while the left lobe measured  $2.24 \pm 0.22$  cm in length and  $1.32 \pm 0.12$  cm in width (Table 1). No statistically significant morphometric differences were observed between the right and left liver lobes in animals ( $p > 0.05$ ), and measurements indicated substantial overlap between lobes in the present study. Contrast-enhanced CT scans provided sharp delineation of hepatic margins and excellent visualization of intrahepatic vascular structures, including central portal and hepatic venous branches. Non-contrast CT images illustrated homogeneous soft-tissue attenuation throughout the hepatic parenchyma, with density values intermediate between those of pulmonary tissue and bone. The 3D reconstructions enhanced anatomical understanding by illustrating vascular branching patterns and verifying the absence of focal lesions, abnormal structures, or asymmetry (Figures 3 and 4; Table 2).

**Table 2.** Liver volume and attenuation/signal intensity in Long-Eared Hedgehogs (*Hemiechinus auritus*) across imaging techniques

Modality	Liver lobe	Volume (mL; Mean $\pm$ SD)	Attenuation / Signal intensity	p-value (Volume)
CT (non-contrast)	Right	$1.92 \pm 0.20$	Homogeneous parenchyma, $52.4 \pm 4.8$ HU	0.18
	Left	$2.01 \pm 0.22$	Similar pattern, $53.9 \pm 5.1$ HU	-
CT (contrast)	Right	$1.95 \pm 0.21$	Homogeneous parenchyma, $103.6 \pm 9.7$ HU	0.17
	Left	$2.04 \pm 0.23$	Homogeneous parenchyma, $99.8 \pm 8.9$ HU	-
CT (3D)	Right	$1.94 \pm 0.19$	Homogeneous parenchyma with clear intrahepatic vessels	0.19
	Left	$2.03 \pm 0.21$	Homogeneous parenchyma; no focal hepatic lesions	-
MRI (non-contrast)	Right	$1.96 \pm 0.20$	Intermediate signal relative to muscle; lower than subcutaneous fat	0.20
	Left	$2.05 \pm 0.22$	Homogeneous parenchymal signal	-
MRI (contrast)	Right	$1.98 \pm 0.21$	Homogeneous enhancement; intermediate relative to muscle; lower than fat	0.19
	Left	$2.07 \pm 0.23$	Homogeneous enhancement with well-defined margins	-

Note: Volume values are presented as mean  $\pm$  standard deviation (SD). CT attenuation values are expressed in Hounsfield units (HU). MRI signal intensity findings are qualitative and reported relative to adjacent tissues. A p-value represents paired comparisons between right and left hepatic lobes within each imaging modality (paired-sample t-tests). Statistical results are interpreted as exploratory due to the small sample size ( $n = 7$ ).

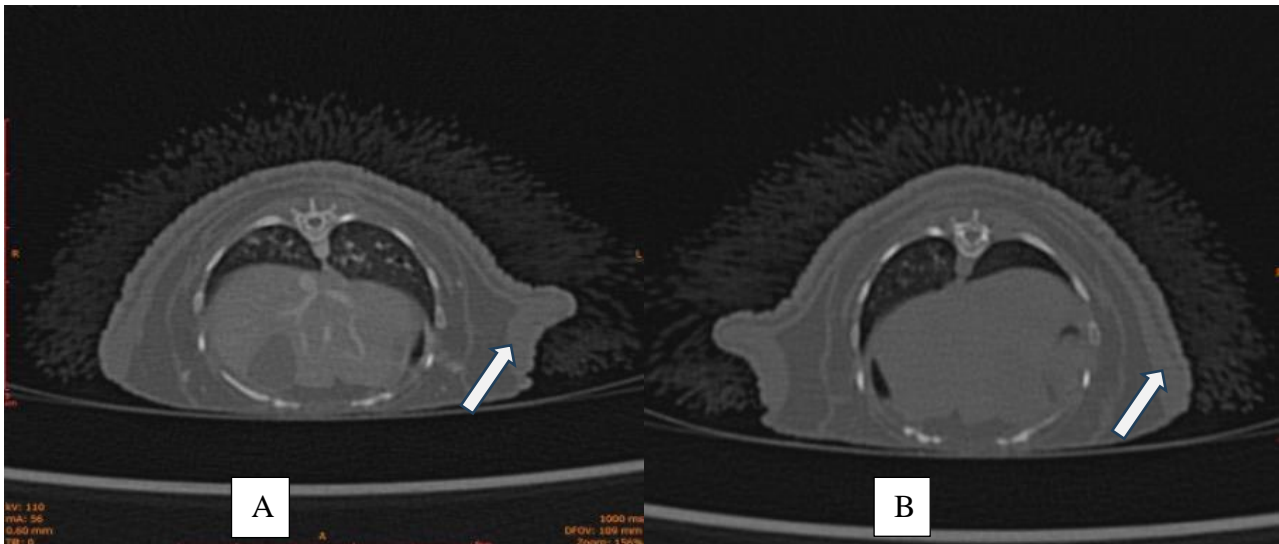


**Figure 3.** Transverse computed tomography (CT) images of the cranial abdomen in an adult male long-eared hedgehog (*Hemiechinus auritus*). **A:** A contrast-enhanced CT image, **B:** A non-contrast CT image. Arrows indicate the liver, visualized as a homogeneous soft-tissue structure in the cranial abdomen.



**Figure 4.** Three-dimensional contrast-enhanced computed tomography (CT) reconstruction of the cranial abdomen in an adult male long-eared hedgehog (*Hemiechinus auritus*). The arrow indicates the liver, showing its overall three-dimensional configuration and the intrahepatic vascular branches visualized after contrast administration.

### Magnetic resonance imaging

Magnetic resonance imaging provided superior soft-tissue contrast compared to the other imaging techniques. On T2-weighted sequences, the hepatic parenchyma appeared hypointense relative to nearby soft tissues, whereas intrahepatic vascular and biliary structures demonstrated hyperintense luminal signals, making them more visible. On T1-weighted sequences, hepatic signal intensity was lower than that of the spleen, which facilitated accurate delineation of lobar margins and the hepatic capsule. Contrast-enhanced MRI sequences demonstrated uniform parenchymal development with signal intensity intermediate between that of skeletal muscle and subcutaneous fat. Hepatic borders were sharply defined, and the lobes exhibited consistent internal structures. Non-contrast MRI sequences illustrated similar morphological features, with no focal parenchymal lesions, vascular abnormalities, biliary dilation, or signal heterogeneity (Figure 5).

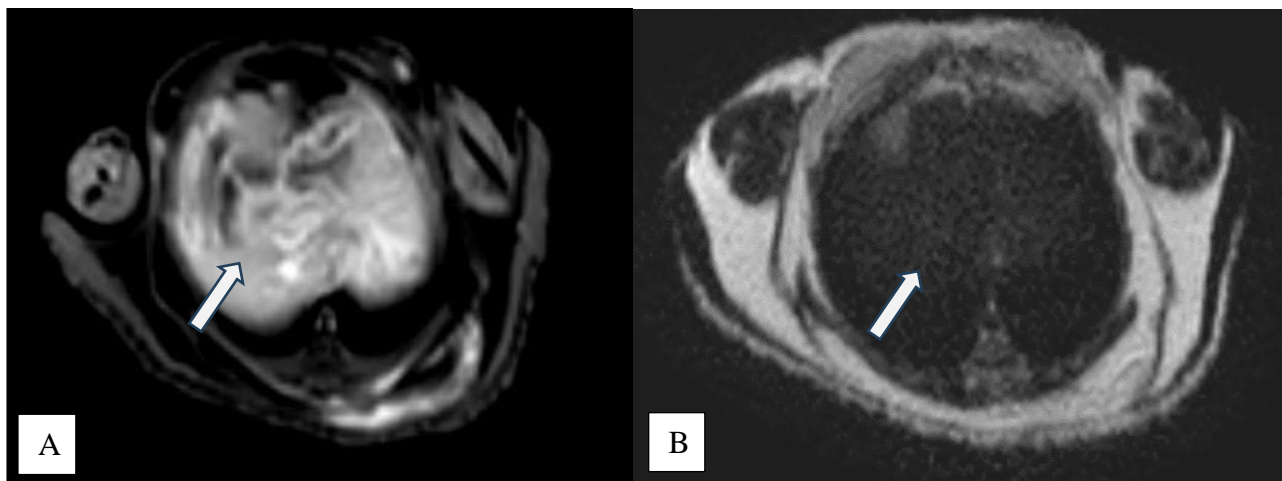


**Figure 5.** Transverse magnetic resonance imaging (MRI) images of the cranial abdomen in an adult male long-eared hedgehog (*Hemiechinus auritus*; aged one year old). **A:** A contrast-enhanced MRI image, **B:** A non-contrast MRI image. Arrows indicate the liver in both panels.

### Comparative morphometric analysis

Morphometric evaluation across all imaging techniques indicated that the right and left hepatic lobes of *H. auritus* had closely similar dimensions, with only slight numerical differences in mean length and width (Table 1). The calculated length-to-width ratios for both lobes were nearly identical, demonstrating considerable overlap and indicating no measurable structural distinction between the two lobes. Quantitative measurements from CT and MRI consistently illustrated similar shapes, highlighting their morphological similarity rather than distinct differences in the lobes. Paired-sample statistical comparisons further supported these observations. No significant differences were detected between the right and left hepatic lobes in length, width, estimated volume, or CT/MRI-derived attenuation and signal characteristics ( $p > 0.05$ ; Tables 1 and 2). Due to the small sample size, these analyses were interpreted as exploratory. Nonetheless, the lack of statistical significance was observed consistently across all techniques. The morphometric results indicated that the liver of the long-eared hedgehog has a mostly symmetrical lobar structure, with no measurable signs of asymmetry. The morphometric suggested there was no evidence of functional differences or species-specific specializations between the liver lobes, indicating a uniform liver structure.

## DISCUSSION

The multimodal imaging approach used in the present study provided a coherent, detailed description of hepatic anatomy in the long-eared hedgehog. Radiography, ultrasonography, CT, and MRI each contributed complementary information, enabling visualization of hepatic margins, parenchymal features, and major vascular landmarks in clinically healthy adult animals.

The radiographic assessment confidently highlighted the hepatic structure in the cranial abdomen, showing a clear separation from neighboring organs. As with other small exotic mammals, radiography provided limited detail of parenchymal structure but remained helpful in assessing the liver's position and overall shape (Sarani et al., 2024). Ultrasonography provided superior resolution of internal hepatic structure, consistently demonstrating homogeneous parenchymal echotexture, visible gallbladder morphology, and well-defined portal and hepatic vasculature. The

ultrasonographic appearance of the hepatic parenchyma, gallbladder, and central vascular structures observed in the present study was consistent with findings reported in African hedgehogs and other small mammals, including rabbits and chinchillas (Taki-El-Deen, 2020; Taati *et al.*, 2024).

The CT imaging further enhanced structural definition, allowing precise delineation of hepatic margins, lobar boundaries, and intrahepatic vascular branching. The observed CT-based anatomical features were consistent with prior findings in chinchillas, ferrets, and rabbits, where non-invasive cross-sectional imaging was highly effective for characterizing visceral morphology (Capello and Lennox, 2013; Karakurum *et al.*, 2024). MRI provided the highest soft-tissue contrast among all imaging techniques, enabling more precise differentiation of lobar boundaries and parenchymal features, especially in areas impacted by partial-volume effects or diaphragm overlap seen on CT. Such advantages of MRI, particularly its superior soft-tissue contrast and reduced susceptibility to overlapping structures compared with CT, are well recognized in veterinary diagnostic imaging across domestic animals, exotic species, and wildlife, regardless of the organ (Zhang *et al.*, 2013; Jones *et al.*, 2020; Greco *et al.*, 2023).

Across all imaging techniques, the right and left hepatic lobes demonstrated closely similar dimensions, volumes, and tissue characteristics. This bilateral symmetry was consistent with published anatomical observations in several small exotic mammals, including ferrets, chinchillas, and African hedgehogs (Capello and Lennox, 2013). The high numerical agreement among measurements was due to the use of standardized anatomical landmarks, repeated measurements, and strong inter-observer reliability, with ICC values between 0.87 and 0.94. These methodological strengths reduced variability and supported the internal consistency of the morphometric dataset.

The species-specific reference values established in the present study provided valuable baseline data for veterinarians assessing liver health in *H. auritus*. Given the limited availability of published imaging data for hedgehogs, which are frequently obtained from diseased cases rather than healthy populations, the current findings enhance the existing diagnostic framework by establishing reference data on normal hepatic dimensions, parenchymal appearance, and vascular patterns across several imaging techniques. The established reference parameters may help clinicians to distinguish normal anatomical variation from early manifestations of hepatic disease.

The present study has some limitations, including a small sample size, which reduced statistical power and might not represent the full biological variability within the species. Only healthy adult males were examined, so age-related, sex-related, or pathological differences could not be assessed. Some images might have been affected by minor motion artifacts, species-specific thoracoabdominal shapes, and varying inflation levels of gastrointestinal structures. Doppler ultrasonography and advanced MRI techniques can provide additional insights into hepatic vascular dynamics, as indicated by previous veterinary imaging studies on abdominal organ perfusion and vascular evaluation (Greco *et al.*, 2023; Karakurum *et al.*, 2024). Comparative studies involving African hedgehogs, chinchillas, rabbits, and ferrets could provide valuable context for understanding hepatic morphology across small exotic mammals, thereby improving the interpretive value of the current findings (Taati *et al.*, 2024; von Stade and Sadar, 2024).

## CONCLUSION

The present study demonstrated that the combined use of radiography, ultrasonography, CT, and MRI provided detailed and complementary evaluations of hepatic anatomy in the long-eared hedgehog (*H. auritus*). Radiography reliably identified the overall position and shape of the liver, ultrasonography allowed dynamic visualization of parenchymal echotexture, the gallbladder, and central vascular structures, CT enabled precise morphometric assessment and clear depiction of lobar boundaries and intrahepatic vasculature, and MRI provided the highest soft-tissue contrast, improving visualization of parenchymal signal patterns and capsular margins. Across all techniques, the right and left hepatic lobes indicated similar dimensions and imaging features, indicating a bilaterally symmetrical liver structure in healthy adult animals. The reference measurements and qualitative imaging features established in the present study provided initial normative data for *H. auritus*, offering a practical diagnostic framework for clinicians evaluating liver health in long-eared hedgehog species. Future studies should investigate larger sample sizes, incorporate diseased individuals, and employ functional imaging techniques such as Doppler ultrasonography or perfusion MRI. The mentioned suggestions would be necessary to expand these baseline observations and enhance diagnostic interpretation in exotic animal practice.

## DECLARATIONS

### Acknowledgements

The authors would like to express their gratitude to the staff of the Diagnostic Imaging Unit, Faculty of Veterinary Medicine, Islamic Azad University, Science and Research Branch, Tehran, Iran, for their technical assistance during

imaging procedures. They also acknowledge the wildlife rehabilitation centers in South Khorasan and Sistan-Baluchestan provinces, Iran, for their cooperation in facilitating access to the animals utilized in the present study.

#### **Authors' contributions**

Mohammad Nasrollahzade Masule conceived and designed the study and supervised the research. Mehdi Ghanaat Pisheh performed radiographic and ultrasonographic imaging. Hassan Gilanpour contributed to anatomical interpretation and manuscript revision. Saied Bokaie assisted with statistical analysis and data interpretation. Siamak Mashhadirafiee conducted CT and MRI imaging and prepared the figures. All authors read and approved the final edition of the manuscript.

#### **Ethical considerations**

All experimental procedures were approved by the Animal Ethics Committee of the Islamic Azad University, Science and Research Branch, Tehran, Iran (Approval Code: IR.IAU.SRB.REC.1403.338). The authors confirm that this manuscript is original, has not been published previously, and is not under consideration elsewhere. No artificial intelligence (AI) tools were used for generating or writing the scientific content of this manuscript. The authors of the present study used Grammarly only for language and grammar refinement after they had fully prepared the scientific content. After using Grammarly assistance, the authors reviewed and edited the manuscript as required and take full responsibility for the content of the manuscript.

#### **Funding**

The present study received no financial support.

#### **Competing interests**

The authors declared no conflict of interest.

#### **Availability of data and materials**

The data supporting the findings of the present study are included in the article and are available from the corresponding author upon reasonable request.

## **REFERENCES**

- Ballard B and Cheek R (2016). Introduction to exotic animal medicine. In: R. Cheek and B. Ballard (Editors), Exotic animal medicine for the veterinary technician. John Wiley & Sons., Hoboken, NJ, USA, pp. 1-2. Available at: <https://www.wiley.com/en-us/Exotic+Animal+Medicine+for+the+Veterinary+Technician%2C+4th+Edition-p-9781119863144>
- Bexton S (2016). Hedgehogs. BSAVA manual of wildlife casualties. British Small Animal Veterinary Association, Gloucester, UK, pp. 117-136. DOI: <https://www.doi.org/10.22233/9781910443316.12>
- Capello V and Lennox AM (2013). Clinical radiology of exotic companion mammals. John Wiley & Sons., Hoboken, NJ, USA, pp. 11-13. Available at: <https://pmc.ncbi.nlm.nih.gov/articles/PMC2797350/>
- Greco A, Meomartino L, Gnudi G, Brunetti A, and Di Giancamillo M (2023). Imaging techniques in veterinary medicine. Part II: Computed tomography, magnetic resonance imaging, nuclear medicine. European Journal of Radiology Open, 10: 100467. DOI: <https://www.doi.org/10.1016/j.ejro.2022.100467>
- Hawkins SJ, Doss GA, and Mans C (2020). Evaluation of subcutaneous administration of alfaxalone-midazolam and ketamine-midazolam as sedation protocols in African pygmy hedgehogs (*Atelerix albiventris*). Journal of the American Veterinary Medical Association, 257(8): 820-825. DOI: <https://www.doi.org/10.2460/javma.257.8.820>
- Jones K, Van Asselt N, Mans C, Hetzel S, and Waller III KR (2020). Use of radiographs and computed tomography for measurement of kidney size in healthy chinchillas (*Chinchilla lanigera*). Journal of Exotic Pet Medicine, 35: 106-111. DOI: <https://www.doi.org/10.1053/j.jepm.2020.04.011>
- Juan-Sallés C and Garner MM (2007). Cytologic diagnosis of diseases of hedgehogs. Veterinary Clinics of North America: Exotic Animal Practice, 10(1): 51-59. DOI: <https://www.doi.org/10.1016/j.cvex.2006.10.003>
- Karakurum E, Dimitrov R, Stamatova-Yovcheva K, Ersen M, and Dilek OG (2024). Anatomical computed tomography and magnetic resonance imaging architecture of the kidneys in the chinchilla (*Chinchilla lanigera*). Indian Journal of Animal Research, 58(5): 785-790. DOI: <https://www.doi.org/10.18805/IJAR.BF-1511>
- Islam MT and Tsnobiladze V (2024). The application, safety, and recent developments of commonly used gadolinium-based contrast agents in MRI: A scoping review. European Medical Journal, 9(3): 63-73. DOI: <https://www.doi.org/10.33590/emj/ZRVN2069>
- Nabipour A and Dehghani H (2012). Light and electron microscopic features of the kidney in hedgehog (*Hemiechinus auritus*). Journal of Veterinary Anatomy, 5(1): 91-106. DOI: <https://www.doi.org/10.21608/jva.2012.44887>

- Sarani S, Enferadi A, Hasani SJ, Sarani MY, Rahnama M, and Sarani F (2024). Identification of zoonotic pathogenic bacteria from blood and ticks obtained from hares and long-eared hedgehogs (*Hemiechinus megalofis*) in eastern Iran. *Comparative Immunology, Microbiology and Infectious Diseases*, 104: 102097. DOI: <https://www.doi.org/10.1016/j.cimid.2023.102097>
- Taati M, Raisi A, Golmirzaei M, and Rashnoei N (2024). Electrocardiogram assessment in long-eared hedgehogs (*Hemiechinus auritus*) following administration of anesthetics. *Veterinary and Animal Science*, 26: 100400. DOI: <https://www.doi.org/10.1016/j.vas.2024.100400>
- Taki-El-Deen F (2020). Comparative anatomical studies on the skull of three mammals in Egypt having different diets. *The Egyptian Journal of Hospital Medicine*, 80(1): 696-703. DOI: <https://www.doi.org/10.21608/EJHM.2020.99345>
- von Stade L and Sadar MJ (2024). Advanced imaging of small mammals. *Advances in Small Animal Care*, 5(1): 51-65. DOI: <https://www.doi.org/10.1016/j.yasa.2024.06.004>
- Zhang JL, Rusinek H, Chandarana H, and Lee VS (2013). Functional MRI of the kidneys. *Journal of Magnetic Resonance Imaging*, 37(2): 282-293. DOI: <https://www.doi.org/10.1002/jmri.23805>

**Publisher's note:** Sciencline Publication Ltd. remains neutral with regard to jurisdictional claims in published maps and institutional affiliations.



**Open Access:** This article is licensed under a Creative Commons Attribution 4.0 International License, which permits use, sharing, adaptation, distribution and reproduction in any medium or format, as long as you give appropriate credit to the original author(s) and the source, provide a link to the Creative Commons licence, and indicate if changes were made. The images or other third party material in this article are included in the article's Creative Commons licence, unless indicated otherwise in a credit line to the material. If material is not included in the article's Creative Commons licence and your intended use is not permitted by statutory regulation or exceeds the permitted use, you will need to obtain permission directly from the copyright holder. To view a copy of this licence, visit <https://creativecommons.org/licenses/by/4.0/>.

© The Author(s) 2025